

X-RAY COMPUTED MICROTOMOGRAPHY APPLIED TO PEARLS: METHODOLOGY, ADVANTAGES, AND LIMITATIONS

Stefanos Karampelas, Jürgen Michel, Mingling Zheng-Cui, Jens-Oliver Schwarz, Frieder Enzmann, Emmanuel Fritsch, Leon Leu, and Michael S. Krzemnicki

X-ray computed microtomography reveals the internal features of pearls with great detail. This method is useful for identifying some of the natural or cultured pearls that are difficult to separate using traditional X-radiography. The long measurement time, the cost of the instrumentation, and the fact only one pearl at a time can be imaged are some of this method's disadvantages.

The value of a pearl is strongly dependent on its natural or cultured origin (for the exact definitions of natural and cultured pearls, see CIBJO, 2010). There are two major categories of cultured pearls: beaded (bead with a mantle-tissue graft; BCPs) and non-beaded (solely a mantle-tissue graft; NBCPs). (For more information regarding grafting and beading, see Sturman [2009] and references therein.)

Traditional X-radiographs are by far the most useful tool to separate cultured from natural pearls (Webster, 1994). Radiographs provide a projection on a plane of the X-ray transparency of the investigated object; typically, the bead or structures related to the tissue used to stimulate growth of the cultured pearl will have a different appearance from that of the pearl itself. In the last decade, however, the market has received large quantities of freshwater as

well as some saltwater NBCPs that are sometimes difficult to identify using radiography (Scarratt et al., 2000; Akamatsu et al., 2001; Hänni, 2006; Sturman and Al-Attawi, 2006; Sturman, 2009; figure 1). Moreover, drilling of pearls may remove the evidence laboratories need to determine their origin (Crowningshield, 1986a,b). Thus, there is a need to improve the acquisition of X-ray images of pearls—for example, through the use of multiple images taken in different directions. Even so, determination of the natural or cultured origin of a small number of pearls remains difficult with radiography alone (see questionable cases in Sturman, 2009). Recently, X-ray computed microtomography has shown promise for pearl identification (Strack, 2006; Wehrmeister et al., 2008; Kawano, 2009; Krzemnicki et al., 2009).

Developed in the 1960s, computed tomography (CT or μ -CT for computed microtomography) allows the user to investigate nondestructively the internal structure of an object with high spatial resolution, providing applications for biology/medicine, materials science, and geology (see Ketcham and Carlson, 2001; Van Geet et al., 2001; Jacobs and Cnudde, 2009). It works by iteratively taking radiographic projections of a rotating sample (usually through 360°; figure 2). X-rays are attenuated by the sample as a function of its thickness and the linear attenuation coefficient (also known as the absorption coefficient—in this case, how easily the material can be penetrated by the X-rays) of the material. Projections of the sample are typically recorded by a CMOS (complementary metal-oxide semiconductor) flat-panel detector with an integrated scintillator. These projections are used to reconstruct three-dimensional (3D) models of the investigated object. Then, two-dimensional (2D) slices can be cut through the 3D models in different directions. Depending on the size of the studied area, it is possible to attain resolutions down to the micrometer scale. Resolution is generally given as

See end of article for About the Authors and Acknowledgments.

GEMS & GEMOLOGY, Vol. 46, No. 2, pp. 122–127.

© 2010 Gemological Institute of America

the length of one pixel, or expressed as a volume element (voxel, a 3D pixel). To be resolved, features must be several voxels in dimension in at least one direction.

In this study, all the results are grayscale—the radiographs as well as the 2D and 3D slices/models. In the radiographic images, lighter colors indicate materials with higher density (e.g., calcium carbonate) and darker colors represent lower-density materials (e.g., organic matter or voids). With longer measurements, the calcium carbonate polymorphs can be separated (e.g., aragonite from calcite and vaterite: see Wehrmeister et al., 2008; Soldati et al., 2009).

MATERIALS AND METHODS

More than 50 samples known to be natural pearls and beaded or non-beaded cultured pearls from various reputable sources were imaged and compared using X-radiography and X-ray μ -CT. This study includes the results for 16 of these samples, representing different pearl categories: 6 natural pearls, as well as 4 beaded and 6 non-beaded cultured pearls (both freshwater and saltwater) from various mollusks. Five were drilled or half-drilled; two were mounted in jewelry (see table 1).

Film X-radiography was performed at the Gübelin Gem Lab, following the standard techniques used in most gemological laboratories (see, e.g., Akamatsu et al., 2001). X-rays were generated by a Comet X-ray unit, and the samples were immersed in a lead nitrate solution (used as scatter-reducing fluid). Two or more radiographs were taken in different directions for all samples. Each image required about 20 minutes.

Microtomography measurements were performed at the Institute of Geosciences of Mainz University, using a ProCon X-Ray CT-Alpha instrument equipped with a YXLON FXE 160.51 X-ray tube and a Hamamatsu flat-panel sensor detector (figure 3). Although this instrument is capable of taking images that are 2048×2048 pixels (50 μ m per pixel), all of the images we used were taken with a setting of 1024×1024 pixels (100 μ m per pixel); that is, four pixels were merged as one during image recording. This procedure allowed for a shorter measurement time and smaller volumes of data, but it halved the given reso-



Figure 1. Some white to yellowish brown (“golden”) pearls are difficult to identify by classical X-radiography, as they present questionable structures. A mixture of natural and cultured pearls (up to ~9.5 mm) are shown here. Photo by Evelyne Murer.

lution. The instrumentation could measure objects as small as 1 mm or as large as ~100 mm wide and 90 mm tall. The highest resolution could be obtained by placing small objects close to the X-ray source; this was done in some cases to more closely examine interesting or questionable structures. So-called region-of-interest (ROI) scans allow imaging of larger objects or magnifications of a specific part of an object. The drawbacks of such scans are typically an increase in artifacts and poorer image quality. The sample chamber is $30 \times 30 \times 30$ cm. Unlike radiography, microtomography can only image one pearl (loose or, in some cases, mounted) at a time, not a strand of pearls.

A series of tests were run to define the ideal parameters for the highest contrast between the different phases in pearls. X-rays were generated with 100 kV accelerating

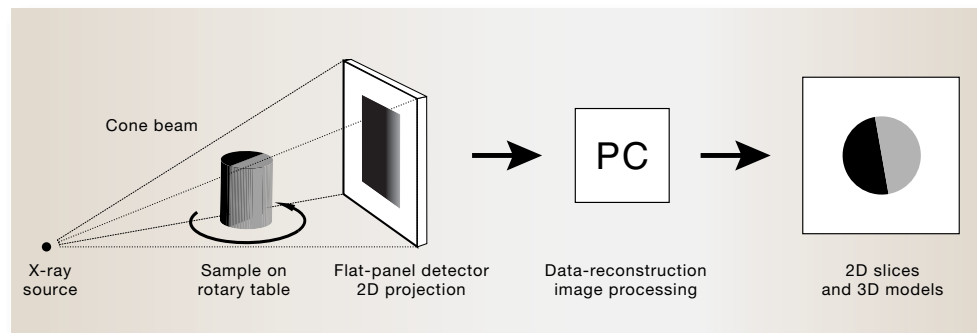


Figure 2. Components of the μ -CT analytical process are shown in this schematic drawing.

TABLE 1. Characteristics and μ -CT resolution of the studied pearl samples.^a

Sample no.	Type	Mollusk	Size (mm)	Shape	Color	Condition	μ -CT resolution (μ m)
SK-61	Natural SW	<i>Pteria spp.</i>	8.7 • 8.1	Drop	Gray-black	Drilled ^b	11.0
SK-46	Natural SW	<i>Pinctada spp.</i>	6.4	Round	Light "cream"	Drilled	7.0
Pp07	Natural SW	<i>Pteria spp.</i>	10.1 • 6.5 • 3.9	Baroque	Light "cream"	Sawn	11.0
GGL03	Natural FW	Unionida order	9.5–10.2 • 7.0	Button	Light gray	Whole	10.8
GGL33	Natural FW	Unionida order	6.9–7.4 • 6.3	Button	White	Whole	8.0
GGL27	Natural FW	Unionida order	6.0	Round	White	Whole	6.4
GGL17	Beaded SWCP	<i>P. margaritifera</i>	9.7	Round	Gray-black	Whole	10.6
GGL18	Beaded SWCP	<i>P. margaritifera</i>	10.4 • 9.9	Drop	Gray-black	Whole	11.3
GGL19	Beaded SWCP	<i>P. maxima</i>	12.7 • 11.3	Button	White	Whole	13.8
GGL32	Beaded FWCP	<i>Hyriopsis spp.</i>	6.9	Round	Light gray	Drilled	7.7
GGL22	Non-beaded SWCP	<i>P. margaritifera</i>	10.6 • 4.9 • 2.8	Baroque	Light gray	Whole	11.0
SK-50	Non-beaded SWCP	<i>P. sterna</i>	7.2 • 5.4 • 4.2	Baroque	Gray-purple	Whole	8.0
SK-51	Non-beaded SWCP	<i>P. sterna</i>	7.2 • 3.9 • 3.5	Baroque	Gray-purple	Whole	8.0
SK-54	Non-beaded FWCP	<i>Hyriopsis spp.</i>	10.0 • 8.8	Drop	Light gray-purple	Half-drilled	11.0
SK-62	Non-beaded FWCP	<i>Hyriopsis spp.</i>	11.0 • 8.9	Drop	Gray-purple	Half-drilled ^b	10.0
GGL26	Non-beaded FWCP	<i>Hyriopsis spp.</i>	6.3 • 6.0	Near round	Yellowish brown	Whole	6.9

^a Abbreviations: FW = freshwater, SW = saltwater, FWCP = freshwater cultured pearl, SWCP = saltwater cultured pearl.

^b Mounted

Figure 3. For microtomography, we used the ProCon X-Ray CT-Alpha instrument based at the Institute of Geosciences of Mainz University. The outer dimensions are 190 • 150 • 100 cm, and the sample chamber is 30 • 30 • 30 cm. The total weight of the instrument is 2.5 tons. Photo by J. Michel.



NEED TO KNOW

- X-ray computed microtomography can reveal the internal structure of a pearl with micrometer-scale resolution.
- The technique is particularly effective for identifying non-beaded cultured pearls.
- Drawbacks include artifacts produced by sample rotation and metal mountings, long measurement time, large data files, costly instrumentation, and the fact that only one pearl at a time can be imaged.

voltage and 110 μ A target current. The beam was prefiltered by 1-mm-thick aluminum foil to reduce beam-hardening effects. Projections were taken with an exposure time of 500 milliseconds. Each measurement consisted of 800 projections (over a 360° rotation), averaging 10 images for each position. Resolution was strongly dependent on the size of the studied area, and ranged from 6.4 to 13.8 μ m per voxel (see table 1).

Reconstruction of the raw data was done using Volex software developed by the Fraunhofer Institute, Germany, and image processing employed Amira software. Data were output as 3D models and 2D slices in the x-, y-, and z-directions. Each sample required about five hours for analysis (including sample mounting, machine set-up, measuring time, and data/image processing). All the calculations were carried out on PCs with >8 GB RAM. The data generated for each pearl consumed >10 GB of disk space.

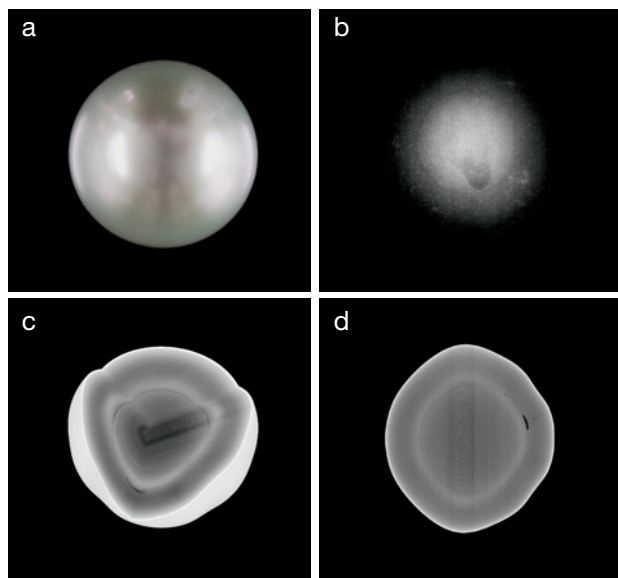


Figure 4. In this (a) white button-shaped beaded saltwater cultured pearl from *P. maxima* (sample GGL19), the bead is visible in the radiograph (b) as well as in the 3D (c) and 2D (d) μ -CT images; however, the boundary between the nacre and the bead is sharper in the μ -CT images, which also show organic matter surrounding the bead. (See also Depository item 1.)

RESULTS AND DISCUSSION

Selected results are shown in figures 4–8 (as well as in the *G&G* Data Depository at gia.edu/gandg), which provide photos of the samples, scans of the X-radiographic films, 3D μ -CT models, and 2D μ -CT slices in the most informative directions. (Note that the scanned films are of lower quality compared to the original films.) For the purpose of visualization, a portion of each 3D model has been removed to show the internal structures. The best structural visualization of the samples is revealed by the 3D μ -CT images. In addition to producing superior image quality, microtomography allows the user to scroll through a pearl virtually by combining the single CT sections into a “movie,” enabling the dynamic recognition of internal structures that are difficult to interpret when observing single CT sections or radiographs (see *G&G* Data Depository for this article and for Krzemnicki et al., 2010).

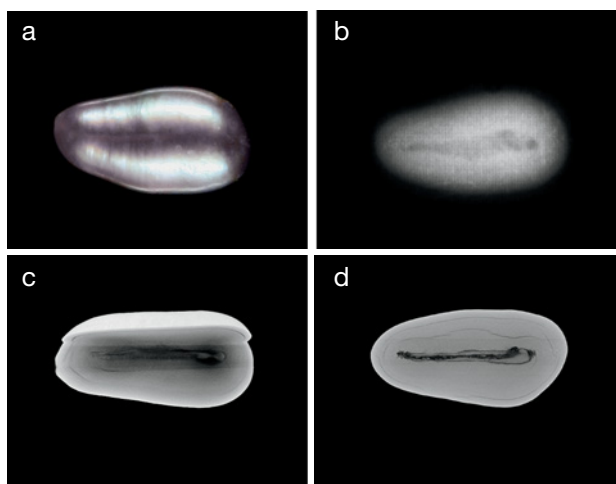
All the beaded cultured pearls as well as all but two of the non-beaded cultured pearls and natural pearls in this study could be identified by radiography. The beads in the BCPs (figure 4), the structures associated with the grafted tissue in the NBCPs (figure 5), and the onion-like layers with a black point in the center of the natural pearls (figure 6) typically were clearly seen in the radiographs. In some cases, however, the μ -CT scans revealed additional characteristics useful for pearl identification. In figure 7, for exam-

ple, it can be seen that a drill hole removed part of the pearl’s central structures, and identification with traditional radiography was uncertain. Although some growth structures appear on the radiograph, the μ -CT images reveal a more detailed and three-dimensional view of the central growth structures that enabled the identification of this pearl as natural. Additional features such as cracks and growth lines were also revealed in some of the μ -CT images. These characteristics were only $\sim 10\ \mu\text{m}$ thick (or less), and were not observed with radiography.

The μ -CT technique does have some limitations. Pearls that are mounted or that have a metal lining within the drill hole may show artifacts, which can mask the internal structures and thus make their identification difficult (figure 8 and Data Depository item 7). In radiographs, the metal mounting is less of an obstacle. Also, μ -CT sections show reconstruction artifacts due to rotation. Although these artifacts can be reduced with appropriate analytical parameters, generally they are not completely removed. The artifacts are manifested as perfectly centered fine circles in horizontal sections (i.e., transaxial sections), and as a blurry rotation axis in the center of the reconstructed image in vertical sections (i.e., sagittal and coronal sections, which are oriented 90° to one another), as illustrated in Data Depository items 1–6. Care must be taken so the fine circles in the transaxial sections are not misinterpreted by an inexperienced observer as (natural) onion-like growth structures.

More structures in natural and cultured pearls observed with μ -CT are well illustrated by Krzemnicki et al. (2010), in the *G&G* Data Depository, and at www.gubelingemlab.ch.

Figure 5. In this (a) gray-purple baroque-shaped non-beaded saltwater cultured pearl from *Pteria sterna* (“keshi”; sample SK-51), tissue-related structures are visible in the radiograph (b) and μ -CT images (c, d). Characteristically, these structures follow the shape of the pearl. Some finer-scale structures are seen in the μ -CT images. (See also Depository item 2.)



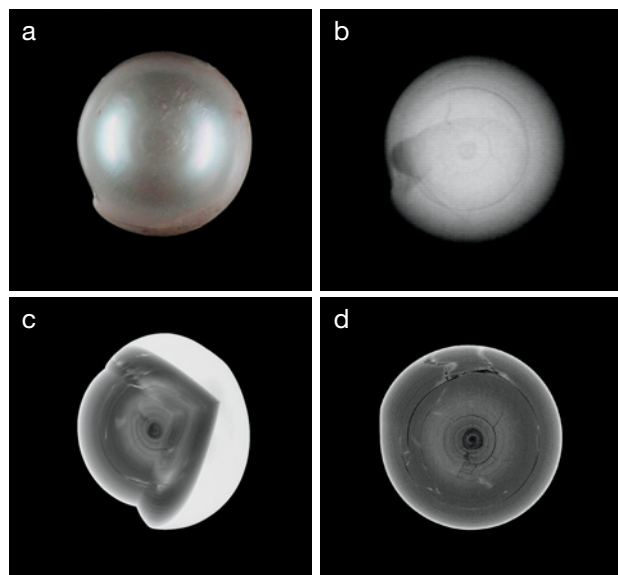


Figure 6. In this (a) light gray button-shaped freshwater natural pearl from the Unionida order (sample GGL03), typical onion-like structures with a black point in the center are visible in the radiograph (b) as well as in the μ -CT images (c, d), but are sharper in the latter. The μ -CT images also reveal fissures surrounded by a denser (white-appearing) material, which are barely visible in the radiograph. (See also Depository item 3.)

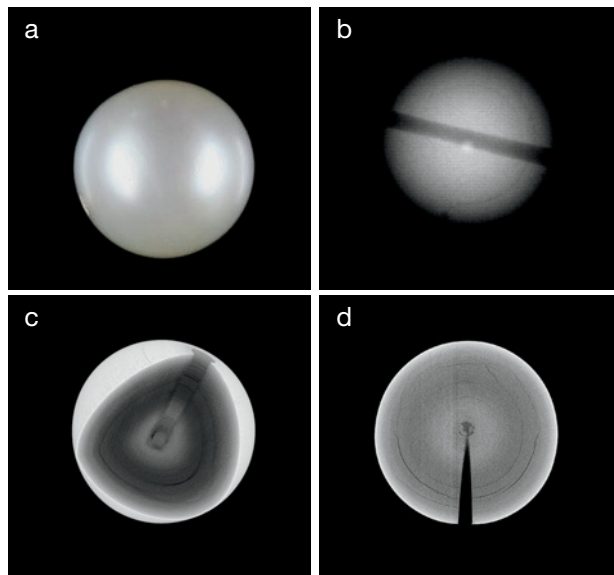
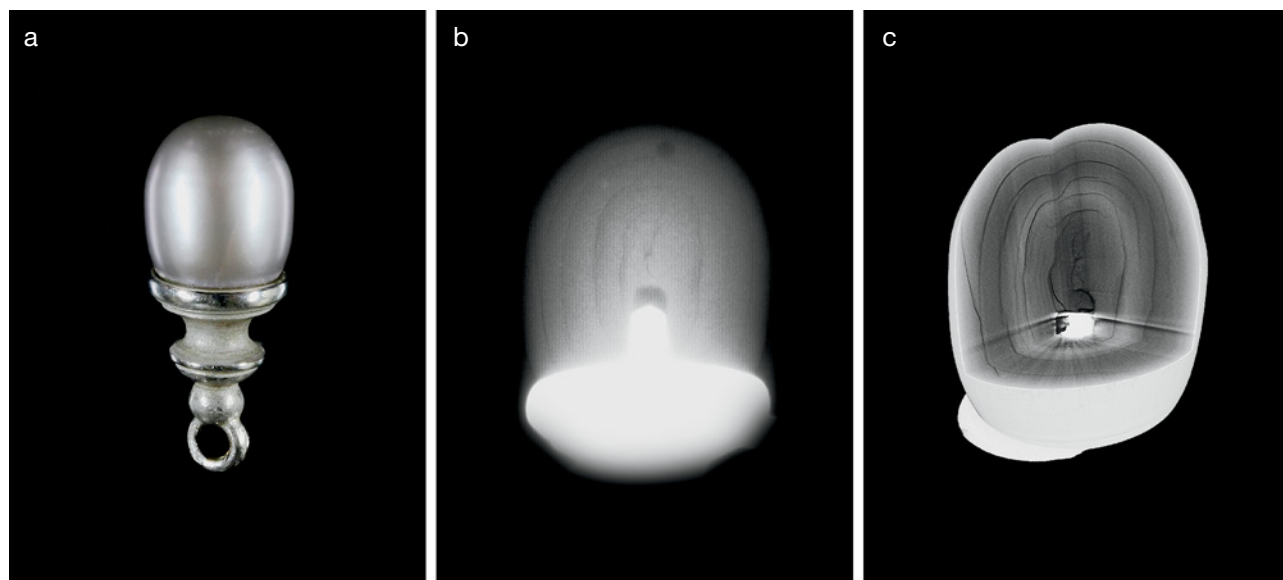


Figure 7. In this (a) drilled, light "cream," round salt-water natural pearl from Pinctada spp. (sample SK-46), concentric growth structures are observed in the radiograph (b), but the drilling has partially removed the structures in the center of the pearl and identification with the radiograph alone is inconclusive. In the μ -CT images (c, d), however, some remnants of the central growth structures are visible, revealing the pearl's natural origin. (See also Depository item 4.)

Figure 8. In this (a) mounted, half-drilled, gray-purple, drop-shaped non-beaded freshwater cultured pearl from Hyriopsis spp. (sample SK-62), characteristic structures of a cultured pearl are observed in the radiograph (b) as well as in the 3D μ -CT image (c). However, in the μ -CT image the metal partially masks the internal structure of the pearl. (See also Depository item 7.)



CONCLUSIONS

Although most cultured and natural pearls can be reliably separated with radiographs alone, their biomineralization is better visualized with X-ray μ -CT (unless they are mounted in metal). In fact, some non-beaded cultured pearls require high-resolution 3D imaging for a correct identification; in such cases, μ -CT can be quite helpful.

The main advantage of tomography is that it gives high-resolution information in three dimensions, whereas radiography condenses the 3D structures onto a flat film as a two-dimensional image. This becomes evident when observing fissures in pearls. Their position within the 3D volume of a pearl is sometimes difficult to interpret in radiographs, even when they are taken in different directions. With μ -CT, the tissue-related structures and the fissures are better revealed, so it is easier to make a correct identification. However, the technique is mainly useful for pearls that do not have metal mountings, it requires a long measurement time, and it consumes a huge amount of data storage space. In addition, μ -CT instrumentation is still costly—about US\$550,000 for the instrument and accessories—and the technique requires scientifically trained staff for analysis and interpretation. Note, though, that a new generation of instruments using X-rays are entering the market, which could be used for digital radiography as well as μ -CT, at the same or even lower prices.

Additional μ -CT studies of problematic pearls (e.g., the non-beaded types described by Sturman, 2009) are expect-

ed to reveal more of the strengths and limitations of this emerging method. Studies at higher resolution, magnifying a specific region of the sample (such as with synchrotron μ -CT), may reveal some very small details of pearl structure that are useful for their identification. Micro-CT analysis may also prove helpful for identifying organic gem materials protected by CITES, such as corals and ivory.

ABOUT THE AUTHORS

Dr. Karampelas (s.karampelas@gubelingemlab.ch) is a research scientist, and Mrs. Zheng-Cui is an analyst, at the Gübelin Gem Lab, Lucerne, Switzerland. Mr. Michel, Dr. Schwarz, and Dr. Enzmann are researchers, and Mr. Leu is an undergraduate student, in the Institute of Geosciences at Johannes Gutenberg University of Mainz, Germany. Dr. Fritsch is professor of physics at the University of Nantes, Institut des Matériaux Jean Rouxel (IMN)-CNRS, Team 6205, France. Dr. Krzemnicki is director of the SSEF Swiss Gemmological Institute, Basel.

ACKNOWLEDGMENTS

The authors thank Thomas Hainschwang (Gemlab, Balzers, Principality of Liechtenstein), Edigem Ltd. (Lucerne, Switzerland), Centre de Recherche Gemmologique (University of Nantes, France), and Perlas del Mar de Cortez (Guaymas, Mexico) for providing some of the study samples, as well as Alessandra Spingardi (Gübelin Gem Lab) for the photos of the samples.

REFERENCES

- Akamatsu S., Zansheng T.L., Moses T.M., Scarratt K. (2001) The current status of Chinese freshwater cultured pearls. *G&G*, Vol. 37, No. 2, pp. 96–113.
- CIBJO (2010) *The Pearl Book: Natural, Cultured & Imitation Pearls—Terminology & Classification*. The World Jewelry Confederation, Milan, Italy, 53 pp., http://download.cibjo.org/10_04_21_CIBJO_Pearl_Blue_Book.pdf.
- Crowningshield R. (1986a) Gem Trade Lab Notes: Pearls with unusual drilling features. *G&G*, Vol. 22, No. 1, pp. 50–52.
- Crowningshield R. (1986b) Gem Trade Lab Notes: Cultured pearls, miscellaneous oddities. *G&G*, Vol. 22, No. 2, pp. 110–111.
- Hänni H.A. (2006) A short review of the use of 'keshi' as a term to describe pearls. *Journal of Gemmology*, Vol. 30, No. 1–2, pp. 51–58.
- Jacobs P., Cnudde V. (2009) Applications of X-ray computed tomography in engineering geology or "looking inside rocks. . ." *Engineering Geology*, Vol. 103, No. 3–4, pp. 67–68.
- Kawano J. (2009) Observation of the internal structures of pearls by X-ray CT technique. *Gemmology*, Vol. 40, No. 478, Issue 7, pp. 2–4 [in Japanese].
- Ketcham R.A., Carlson W.D. (2001) Acquisition, optimization and interpretation of X-ray computed tomographic imagery: Applications to the geosciences. *Computers & Geosciences*, Vol. 27, No. 4, pp. 381–400.
- Krzemnicki M.S., Friess S., Chalus P., Hajdas I., Hänni H.A. (2009) New developments in pearl analysis: X-ray micro tomography and radiocarbon age dating. *Journal of the Gemmological Association of Hong Kong*, Vol. 30, pp. 43–45.
- Krzemnicki M., Friess D., Chalus P., Hänni H.A., Karampelas S. (2010) X-ray computed microtomography: Distinguishing natural pearls from beaded and non-beaded cultured pearls. *G&G*, Vol. 46, No. 2, pp. 128–134.
- Scarratt K., Moses T., Akamatsu S. (2000) Characteristics of nuclei in Chinese freshwater cultured pearls. *G&G*, Vol. 36, No. 2, pp. 98–109.
- Soldati A.L., Jacobi D.E., Wehrmeister U., Hofmeister W. (2008) Structural characterization and chemical composition of aragonite and vaterite in freshwater cultured pearls. *Mineralogical Magazine*, Vol. 72, No. 2, pp. 577–590.
- Strack E. (2006) *Pearls*. Rühle-Diebener Verlag, Stuttgart, Germany, 707 pp.
- Sturman N. (2009) The microradiographic structures on non-bead cultured pearls. GIA Thailand, Bangkok, November 21, www.giathai.net/pdf/The_Microradiographic_structures_in_NBCP.pdf [date accessed: Dec. 2, 2009].
- Sturman N., Al-Attawi A. (2006) The "Keshi" pearl issue. *G&G*, Vol. 42, No. 3, p. 142.
- Van Geet M., Swennen R., Wevers M. (2001) Towards a 3D petrography: Application of microfocus computer tomography. *Computers & Geosciences*, Vol. 27, No. 9, pp. 1091–1099.
- Webster R. (1994) *Gems: Their Sources, Description and Identification*, 5th ed. Rev. by P. G. Read, Butterworth-Heinemann, Oxford, UK, 1026 pp.
- Wehrmeister U., Goetz H., Jacob D.E., Soldati A.L., Xu W., Duschner H., Hofmeister W. (2008) Visualization of the internal structure of freshwater cultured pearls by computerized X-ray microtomography. *Journal of Gemmology*, Vol. 31, No. 1–2, pp. 15–21.